UC Davis
UC Davis Previously Published Works

Title

Investigation of the formation and energy density of high-current pulsed electron beams

Permalink

Journal

ISSN

Authors

Daichi, Yoshiaki
Wang, ZHIGANG
Yamazaki, Kazuo
et al.

Publication Date

2007

DOI

Peer reviewed

Investigation of the formation and energy density of high-current pulsed electron beams

Yoshiaki Daichi[a], Zhigang Wang[b], Kazuo Yamazaki[b], Sadao Sano[a]

[a]Sodick Co. Ltd, 3-12-1 Nakamachidai, Tsuzuki-ku,Yokohama, 224-8522, Japan

[b]Department of Mechanical & Aeronautical Engineering, University of California, Davis,

One Shields Avenue, Davis, CA, 95616, USA

Abstract: High-current pulsed electron beams (HCPEB) irradiation is a new potential method to polish hard steels and alloys. After HCPEB machining, the performance of machined surface, such as corrosion resistance and micro-structure, has been greatly improved. Because of its good performance, HCPEB irradiation is playing more and more important roles in polishing hard steels and alloys. However, it is not clear about the energy density of HCPEB under different beam conditions. In this study, experiments have been conducted to investigate the formation of HCPEB and its energy density. Then, effects of argon gas pressure and the applied voltage to solenoid coil on the formation of HCPEB are analyzed. Finally, a mathematical model is developed to describe the relationship between five dominant beam parameters with the energy density of HCPEB, which has a good accuracy in comparison to the experimental results.

Keywords: plasma, electron beam, energy density, nonlinear regression

1. Introduction

Recently, high-current pulsed electron beams (HCPEB) are used for materials processing [1-3]. This treatment not only smoothes surface profiles, but also substantially improves the corrosion resistance and the fatigue characteristics of machined parts [2, 3]. This technique would be a potential machining method for polishing hard die/mold tools. From previous basic studies, it

1

was found that the spatial intensity of HCPEB is inherently distributed non-uniformly, and this non-uniform intensity seems to be inevitable no matter what beams parameters are used. Even for an ideal pure metal irradiated by HCPEB with an imposed uniform spatial intensity distribution, the boundary effect will still cause a non-uniform transverse temperature distribution in the heat affected area. Bretagne et al [4] calculated the electron-energy distribution tails in high pressure EB generated argon plasmas. Recently, Sigeneger and Winkler [5] theoretically investigated the helium plasma in a hollow cathode discharge by a new hybrid approach, and they found significant difference in shapes of the density profiles for the excited atoms considered in their study. In addition, Konstantinov and Khmel [6] used a probe technique to measure the electron temperature and density. Up to now, limited research has been done to determine instantaneous values of the HCPEB. In this work, experiments have been carried out to investigate the formation of HCPEB and measure the energy density of HCPEB, and then a nonlinear regression method is used to fit the energy density model.

2. Experimental methodology

2.1 Generation of high-current pulsed electron beams

A high energy density HCPEB is generated as shown in Fig. 1 [1]. The workpiece is mounted on a worktable inside a vacuum chamber, which is firstly evacuated to 0.03 Pa, thereafter argon gas is added until the inside air pressure reaches 0.05 Pa. Then, a pulse current is supplied into the solenoid coil to generate a magnetic field between the cathode and target material. The diameters of the anode and cathode are 120mm and 60mm, respectively. When the magnetic field reaches its highest strength, a pulse voltage (around 4.0 kV) is applied to the anode. Then, the high current reflected (Penning's) discharge at the anode ionizes the nearby argon gas. Under the effect of the magnetic field generated by the solenoid coil, electrons move spirally and

collide with argon gas atoms. Due to the repetitious collisions with the moving electrons, argon gas atoms are further ionized, which generates plasma near the anode. Owing to its high conductivity, the plasma has a potential close to the anode potential. When the plasma intensity reaches its maximum value, an accelerating pulsed voltage is applied to the cathode. The electric field is localized within the cathode layer of ion space charge, whose length is much less than the cathode-anode gap space [7, 8]. As a result, the electric filed at the cathode reaches a high value (generally, greater than 100kV/cm), and explosive electron emission is initiated at the cathode, resulting in the formation of dense plasma blobs that constitute an electron emitter [8]. Once explosive emission has been initiated, the accelerating voltage is localized with the double layer between the cathode plasma and anode plasma. Finally, the electron beams in the double layer is transported through the anode plasma to a collector (workpiece in the EBM machine).
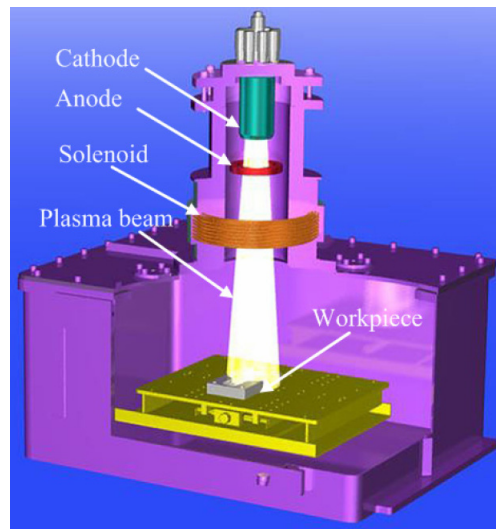

Fig. 1. A schematic illustration of the HCPEB machine [1].

2.2 Experiment setup for capturing the plasma formation

The general description of the experimental setup for measuring the formation of HCPEB is shown in Fig. 2. An inclined mirror is placed at a position where the workpiece is, and then CCD camera captures the images of discharge glow through the mirror. The main parts of the

setup include a pulse generator, a controller, two CCD cameras and a computer. First, the anode trigger signals are input to pulse generator to provide time series signals for the controller. After receiving trigger signals, the controller sends pulse signals to the camera to trigger it to start capturing images. The captured images are stored in a computer via the controller. In this study, a high-speed framing CCD camera C7977-01 provided by Hamamatsu Co. Japan was used, which has a resolution of 1,000,000 pixels and a fast frame rate up to 3.333×10^6 frame per second (fps). As shown in Fig. 2 (b), the interval between the pulse signals to trigger two CCD cameras is a pulse duration, which is 1μs in this paper. Thus, formation of HCPEB can be recorded continuously with these two cameras.
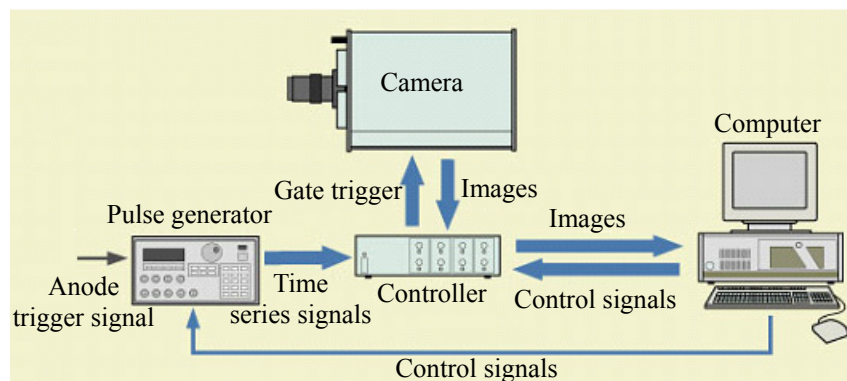
(a) Schematic diagram of measuring system
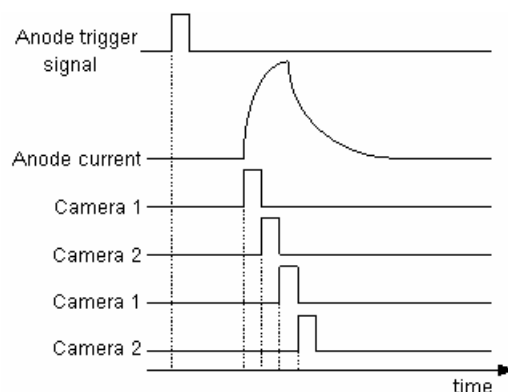
(b) Time series signals to trigger the anode and two CCD cameras

Fig. 2 Experimental setup for measuring the formation of HCPEB

2.3 Experiment design to measure the energy density of HCPEB

4

To ensure effective results, the design of experimental techniques was used to plan the experiments efficiently to measure the energy density of HCPEB. Then, the data collected during experiments was analyzed with the statistical approach. Recently, powerful software has been developed and used in data statistical analysis. With the help of such software, it becomes much easier and more convenient to analyze experimental data. So the main concern for experiments is the experimental design. Apart from factorial designs, response surface methodology (RSM) is another widely used method for experimental designs, which has been used in this study. RSM is a combination of mathematical and statistical techniques used in an empirical study of model building and optimization. In many real applications, two-order response surface is required to be fitted. The central composite design is one of the best choices for fitting a second-order surface [9]. The central composite design is built-up from the factorial designs by adding several center points. Therefore, by choosing a proper number of center points, the efficient estimation of the pure quadratic terms can be controlled, and then a model of the response surface with independent input variables is obtained with regression analysis.

For the energy density measuring experiments, five dominant factors (cathode voltage, anode voltage, solenoid voltage, argon gas pressure in the vacuum, and irradiation distance which is defined as the distance from the center line of the last turn of the solenoid coil to the target material along the beam propagation) are considered in the planning of the experiments. The range of values of each factor was set at three levels, namely low, medium and high levels, as shown in Table 1, which were selected based on the present day manufacturing requirements and allowed range of beam conditions. Under this setting, a 3^5 full factorial design was used so that all the interactions between the independent variables could be investigated. The condition at the center point of factorial design is repeated four times for RSM analysis. Based on this,

totally 243 test conditions of HCPEB irradiation were carried out, and at each beam condition, the irradiation test was repeated three times in order to eliminate the experimental error.

Table 1 Parameters related to E-beam conditions and their values

Variables		Values of different levels		
Designation	Description	Low(−)	Medium(0)	High(+)
Ar	Argon air pressure(Pa)	0.05	0.08	0.12
So	Solenoid voltage(kV)	1.00	1.50	2.00
An	Anode voltage(kV)	3.00	4.00	5.00
Ca	Cathode voltage(kV)	15.0	22.5	30.0
Id	Irradiation distance (mm)	30.0	45.0	60.0

Faradey cup is normally used to measure current, then the energy density can be obtained by integrating of current density multiplied with the voltage. However, it is difficult to directly to use measured current from Faradey cup to estimate the energy density accurately, because some kinetic energy of electrons may be transferred to plasma oscillations or scattered laterally during the acceleration of electrons. Therefore, in this study, a calorimeter with thermal resistors is used to measure the energy densities, as shown in Fig. 3. The calorimeter has a diameter of 120 mm, and nine thermal resistors are placed on it at nine different positions so as to measure the radial distribution of beam energy densities. Based on the temperature measured by the thermal resistors, the beam energy density is calculated.

3. Observation of the formation of HCPEB

In this section, the formation of HCPEB has been observed, and the effects of Ar gas pressure and solenoid voltage on the formation of HCPEB have also been investigated. Figure 4 shows the formation of plasma in the vacuum chamber when So = 1.5kV, An = 5kV, Ca = 0, and Ar = 0.05Pa. Initially, the maximum of the ionization rate is observed near to the wall of the plasma

generation chamber. As shown in Fig. 1, a hollow anode is used to accelerate the electrons, which accelerates those electrons near the anode wall. These faster electrons increase the ionization of argon gas atoms near the anode. Due to the ionization of argon gas atoms, there exist some ion-electron pairs in the plasma generation chamber. These additional ions and electrons can gain energy from the electric field and contribute also to the enhancement of the total ionization. That is why the faster electrons distribute more uniformly inside the chamber gradually after 24 μs.
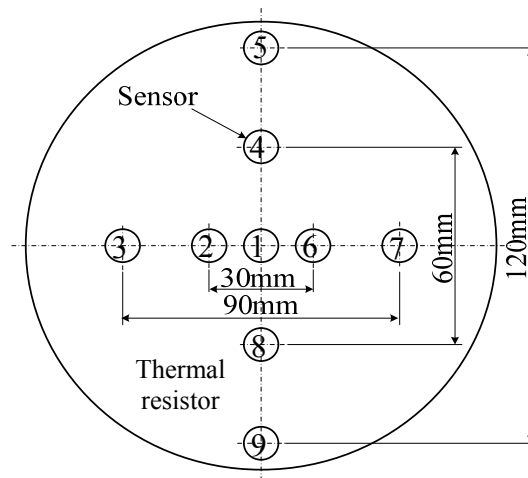

Fig. 3 The structure of calorimeter for measuring energy density of HCPEB

From preliminary experimental studies, it was found that the effect of anode voltage on the beam energy density is less than the solenoid voltage and argon gas pressure. Thus, this paper mainly focused on the effects of solenoid voltage and argon gas pressure on plasma formation. The plasma formation after every 10 μs under different argon gas pressure is shown in Fig. 5. Electron impact ionization of argon atoms was the dominant process of electron production for all the conditions investigated here. Figure 5 shows that the ionization process in the discharge increases with the decrease of argon gas pressure. Since with the decrease of argon gas pressure, the length of plasma generation area increases, this causes an increase of ionization of argon gas atoms. Similar results have also been found in [10]. When the argon gas pressure is 0.20 Pa, the

plasma is only focused on some small areas, because the short duration of the anode voltage, even after 30 μs, the plasma still cannot distribute uniformly. Therefore, large argon gas pressure is not preferred in order to get uniformly distributed HCPEB.
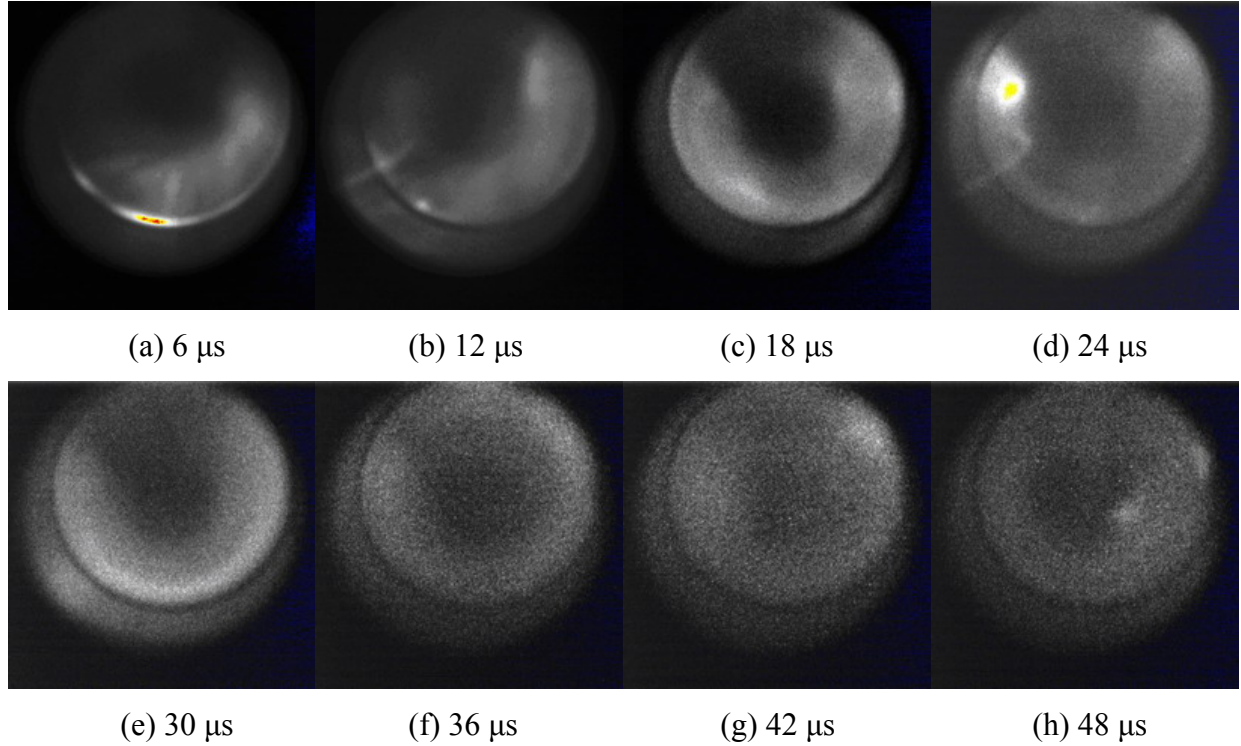

| (a) 6 μs | (b) 12 μs | (c) 18 μs | (d) 24 μs |

| (e) 30 μs | (f) 36 μs | (g) 42 μs | (h) 48 μs |

Fig. 4 Formation of plasma when $So = 1.5kV$, $An = 5kV$, $Ca = 0$, $Ar = 0.05Pa$

As mentioned in Section 2.1, the solenoid coil is mainly used to generate a magnetic field, which makes the electrons move spirally. In this study, the solenoid coil is made of a conducting copper wire, and the diameter of the solenoid coil is 197 mm. The coil has a length of 782 mm and 270 turns and the resistance of the total copper wire is equal to 7.5 Ω. Physically, solenoid magnetic field depends on the permeability of the core, the solenoid length and the current in it. In this study, the first two parameters almost keep constant, and the current in the solenoid is the only changing parameter, which only depends on the voltage applied to the copper wire according to Ohm's law. Therefore, in this study, the changing values of solenoid magnetic field only depend on the applied solenoid voltage. It is reasonable to choose solenoid voltage as a

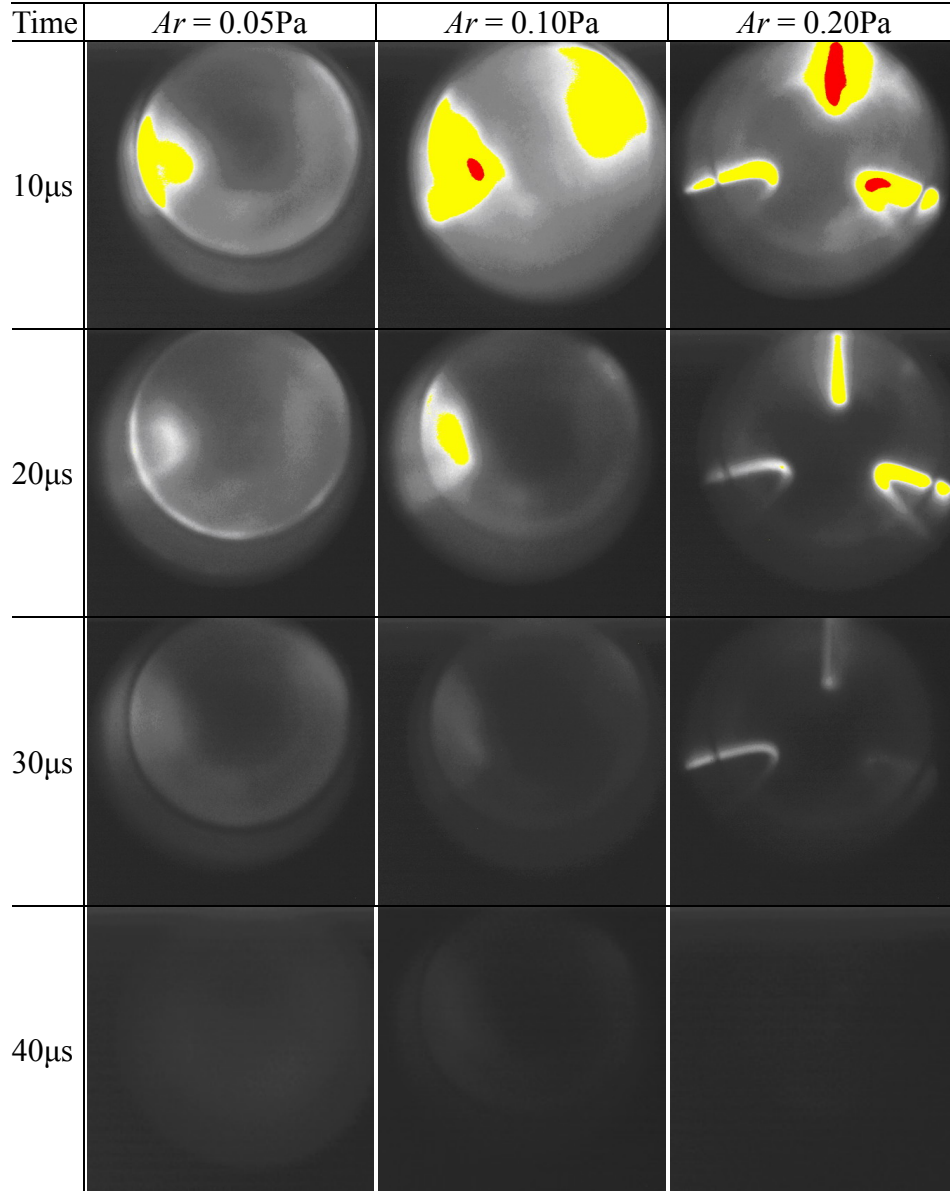| Time	Ar = 0.05Pa	Ar = 0.10Pa	Ar = 0.20Pa
10μs			
20μs			
30μs			
40μs			

Fig. 5 Plasma formation process under three different argon gas pressures

parameter to investigate how solenoid magnetic field affects the formation of HCPEB. The

plasma formation after every 10 μs is shown in Fig. 6 under the beam conditions of An =5kV,

Ca = 0, Ar = 0.05Pa and different solenoid voltages. At a lower solenoid voltage of 0.5 kV,

initially the plasma distributes more uniformly. But after 20 μs, the plasma density at a lower

solenoid voltage seems to be lower too. Because of the lower solenoid voltage, the magnetic

forces applied on electrons are smaller, which causes low moving speed of electrons. Finally, the

ionization of argon gas atoms is low. At high solenoid voltage of 2.0 kV, a strong magnetic field is generated, and the ionization rate is much higher at the beginning because of the faster movement of electrons under strong magnetic field. However, the uniformity of the plasma is worse than that under lower solenoid voltage. Figure 6 shows that uniform plasma with certain density has been created at a solenoid voltage of 1.5 kV.

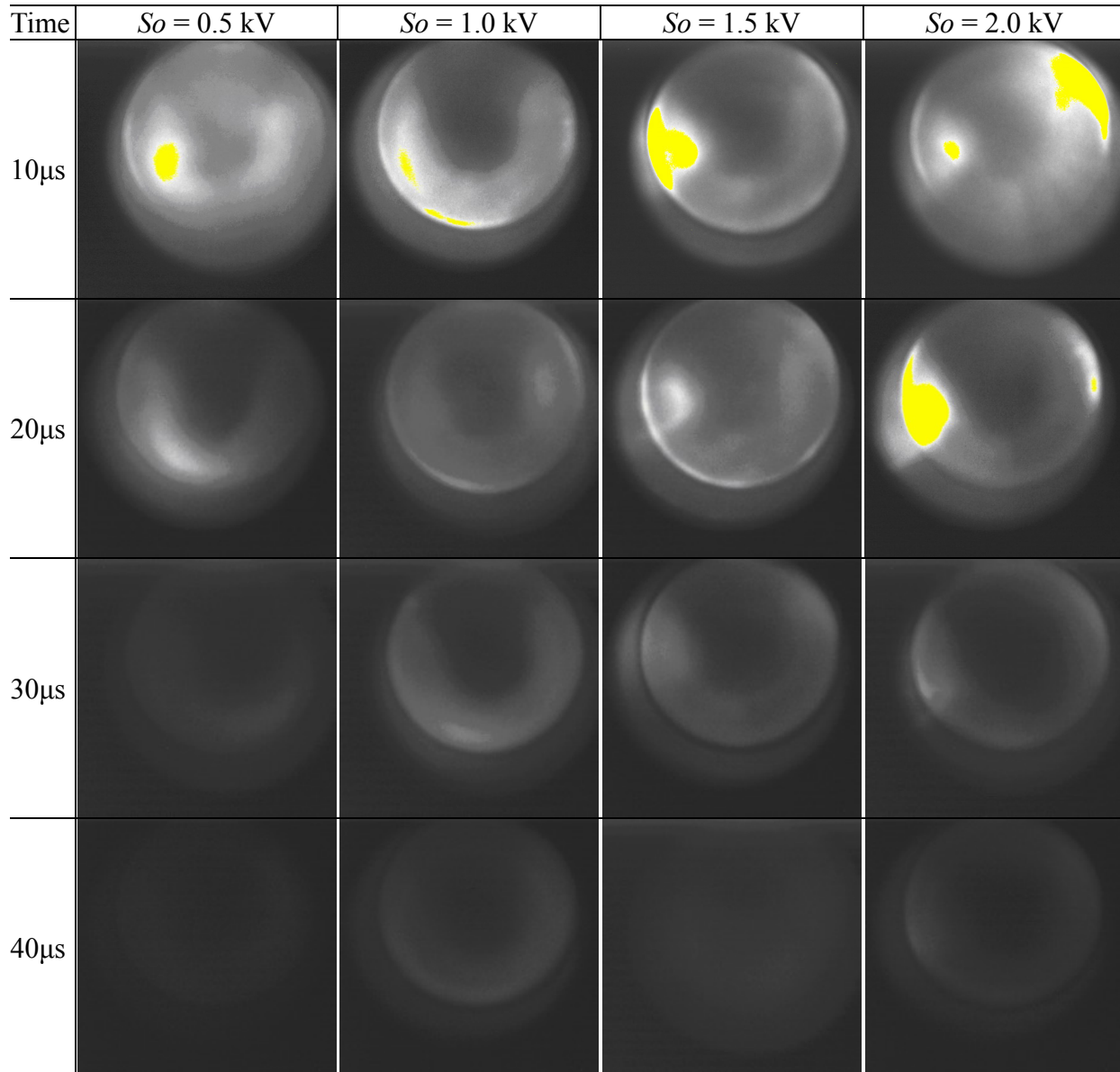| Time	*So* = 0.5 kV	*So* = 1.0 kV	*So* = 1.5 kV	*So* = 2.0 kV
10μs				
20μs				
30μs				
40μs				

Fig. 6 Plasma formation process under four different solenoid voltage

4. Nonlinear regression of the energy density model

Figure 7 shows the measurement result of energy density of 3 irradiation shots using a calorimeter under the beam condition at Ca = 22.5 kV, An = 5.0 kV, So = 1.5 kV, Ar = 0.05 Pa and Ir = 30 mm. From Fig. 7, it can be seen that the energy density reaches its maximum value at the center of the beam. With the increase of the distance away from the center point, the energy density decreases gradually. However, the energy density within an area with a diameter of 40-50 mm is high enough to melt or evaporate metal surface instantly. Therefore, the effective diameter of HCPEB used in this study can be considered as around 40-50 mm. In Section 3, it is found that the glow in the central part is weak. Thus, the distribution of the glow does not correlate to energy density distribution obtained by the calorimeter. Under the effect of applied magnetic field, electrons in the plasma tend to move towards the central part of solenoid coil because the magnetic field reaches its maximum there. This is a possible reason why the energy density in the central part of solenoid coil has a higher intensity.
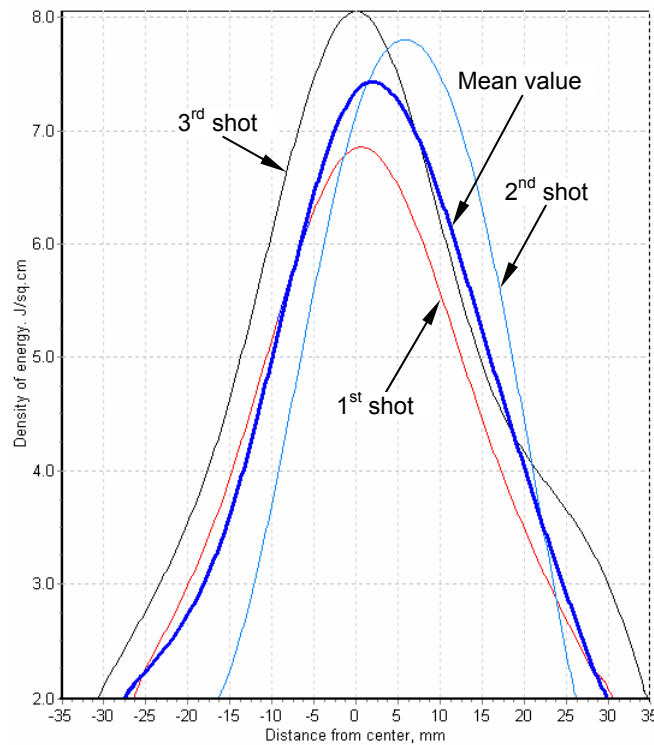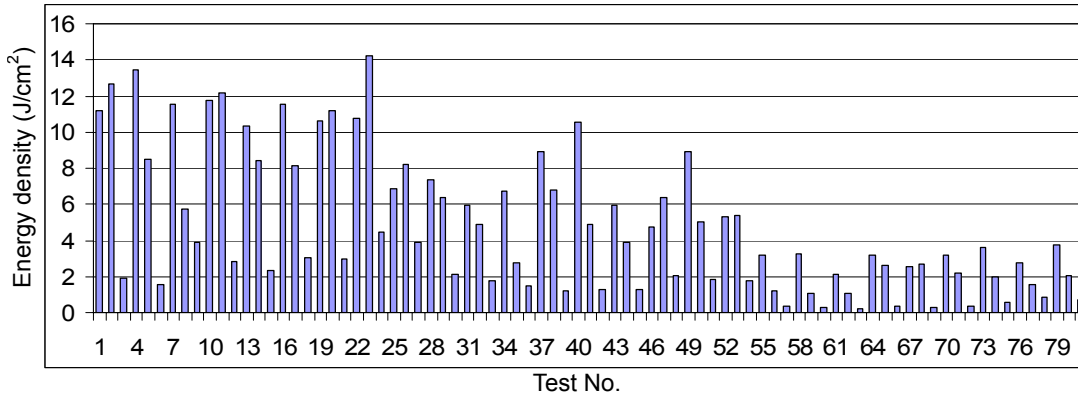

Fig. 7 Energy density distribution of 3 irradiation shots

11

Figure 7 indicates that energy density seems to have a normal distribution with an expectation of 0. If its variation is known, the energy density distribution can be estimated. For simplification, the energy density at the center of calorimeter is considered to derive an energy density model.

(a) Irradiation distance of 30 mm
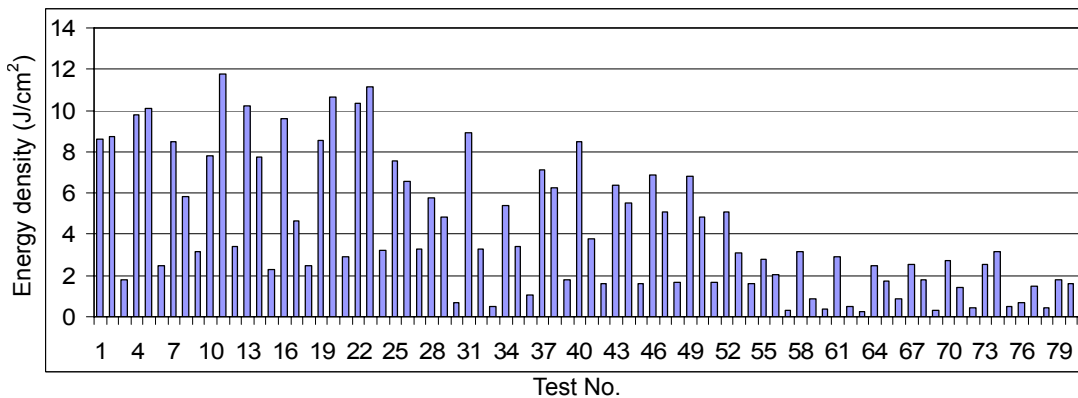
(b) Irradiation distance of 45 mm
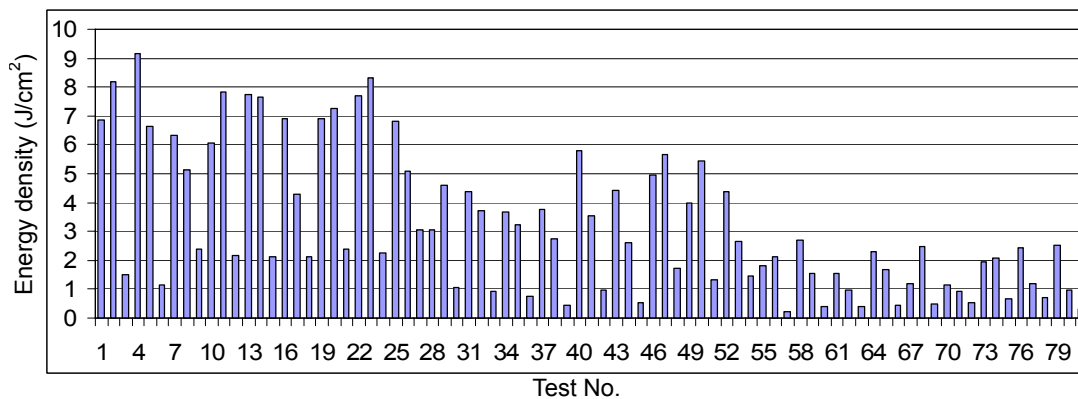
(c) Irradiation distance of 60 mm

Fig. 8 Energy densities at the center of calorimeter under three different irradiation distances

Figure 8 presents the mean values of three irradiation shots under 81 different beam conditions and three different irradiation distances. Under each irradiation distance, the beam conditions are given in Table 2. By comparing the data listed in Fig. 8 (a), (b) and (c), it is found that the energy density decreases with the increase of irradiation distance. At the same time, the energy density also decreases with the decrease of cathode voltage.

Table 2 Beam conditions at different irradiation distance

Test No.	ar	so	an	ca	Test No.	ar	so	an	ca	Test No.	ar	so	an	ca
1	−	+	+	+	28	−	+	+	0	55	−	+	+	−
2	0	+	+	+	29	0	+	+	0	56	0	+	+	−
3	+	+	+	+	30	+	+	+	0	57	+	+	+	−
4	−	−	+	+	31	−	−	+	0	58	−	−	+	−
5	0	−	+	+	32	0	−	+	0	59	0	−	+	−
6	+	−	+	+	33	+	−	+	0	60	+	−	+	−
7	−	0	+	+	34	−	0	+	0	61	−	0	+	−
8	0	0	+	+	35	0	0	+	0	62	0	0	+	−
9	+	0	+	+	36	+	0	+	0	63	+	0	+	−
10	−	+	0	+	37	−	+	0	0	64	−	+	0	−
11	0	+	0	+	38	0	+	0	0	65	0	+	0	−
12	+	+	0	+	39	+	+	0	0	66	+	+	0	−
13	−	−	0	+	40	−	−	0	0	67	−	−	0	−
14	0	−	0	+	41	0	−	0	0	68	0	−	0	−
15	+	−	0	+	42	+	−	0	0	69	+	−	0	−
16	−	0	0	+	43	−	0	0	0	70	−	0	0	−
17	0	0	0	+	44	0	0	0	0	71	0	0	0	−
18	+	0	0	+	45	+	0	0	0	72	+	0	0	−
19	−	+	−	+	46	−	+	−	0	73	−	+	−	−
20	0	+	−	+	47	0	+	−	0	74	0	+	−	−
21	+	+	−	+	48	+	+	−	0	75	+	+	−	−
22	−	−	−	+	49	−	−	−	0	76	−	−	−	−
23	0	−	−	+	50	0	−	−	0	77	0	−	−	−
24	+	−	−	+	51	+	−	−	0	78	+	−	−	−
25	−	0	−	+	52	−	0	−	0	79	−	0	−	−
26	0	0	−	+	53	0	0	−	0	80	0	0	−	−
27	+	0	−	+	54	+	0	−	0	81	+	0	−	−

After getting energy density values from experiments, a nonlinear regression is used to fit the model. Initially, we do not have any idea as to the true model but simply believes that the model is nonlinear. So first, linear terms are used as a starting point for the selected five factors [11], then the nonlinear terms of these five factors can be estimated as the following equation:

$$En = (b_1 ca^2 + b_2 ca) \frac{id \cdot e^{ar^2 - b_4 ar}}{id^2 + b_3 id} (1 - b_5 \ln \frac{an}{2})[1 + (\frac{so - 0.5}{1.5})^{b_6}] \tag{1}$$

Before fitting the model, a set of starting values of these six parameters (b_1, b_2, …, b_6) must be chosen. In this investigation, a starting value grid was tried using SAS NLIN procedure[12]. With this value grid, the initial residual sum of squares for all combinations of starting values was calculated. The "best" starting value is the point that corresponds to the smallest value of the residual sum of squares. Then, this best set of these parameters is selected as the initial value for the following iterations of nonlinear regression. In order to decrease the correlation between estimated parameters, Levenberg-Marquardt method has been used to calculate the derivatives. After fitting the model with the experimental data using PROC NLIN [12], the results of nonlinear regression of the energy density (*En*) model were shown in Table 3. The calculated F-value is 600.9714 for this model. While, the tabulated value of F-value $F_{6, 242}(0.01)$ is only 2.802 by looking up the tables of the F-distribution. So the calculated value is much greater than the tabulated one. Therefore, the results of ANOVA indicate that the main effects of beam conditions (*Ar*, *So*, *An*, *Ca*, *Ir*) are significant at 99% confidence level. As the nonlinear model has high predictability, it is accurate enough to represent the energy density response.

The estimates of these six parameters are also presented in Table 3, together with their associated asymptotic standard error, and the upper and lower values for the asymptotic 95% confidence interval. All results in nonlinear regression are asymptotic.

The correlations among the estimated parameters are presented in Table 4. The correlation

indicates that if the value of a specific parameter changes, other parameters will also change accordingly. If the correlations are very high, the fit of the model may be negatively affected by this. In this nonlinear regression, the highest value of correlation happened between b_1 and b_3 is around 0.7, which is less than the threshold of high correlation (0.80) [12]. Thus, the Levenberg-Marquardt method can fit the model with a good accuracy.

Table 3 Non-linear least squares summary statistics of the energy density model

Source	DF	Sum of Squares	Mean Square	F Value	Approx Pr > F
Regression	6	6019.8186335	1003.3031056	600.9714	<0.0001
Residual	237	395.6641729	1.6694691		
Uncorrected Total	243	6415.4828063			
Corrected Total	242	2468.6821310			

Parameter	Estimate	Asymptotic Std. Error	Confidence Interval (95 %)	
			Lower	Upper
b_1	0.9157122	0.147245050	0.625632232	1.205792095
b_2	2.0188452	2.110862372	-2.13965666	6.177347003
b_3	34.866088	8.384351809	18.34850626	51.38367029
b_4	14.568868	0.772865092	13.04628630	16.09145016
b_5	-0.024771	0.077017222	-0.17649868	0.126956687
b_6	0.3588632	0.093999964	0.173678662	0.544047691

Table 4 Asymptotic correlation matrix of the estimated parameters

Corr.	b_1	b_2	b_3	b_4	b_5	b_6
b_1	1	-0.418731	0.701152	0.308191	-0.326588	0.107689
b_2	-0.418731	1	0.107829	0.047396	-0.050226	0.016561
b_3	0.701152	0.107829	1	-2.4992E-14	-1.3956E-14	-7.9406E-15
b_4	0.308191	0.047396	-2.4992E-14	1	-3.3421E-15	-1.3469E-15
b_5	-0.326588	-0.050226	-1.3956E-14	-3.3421E-15	1	5.1371E-16
b_6	0.107689	0.016561	-7.9406E-15	-1.3469E-15	5.1371E-16	1

Finally, the energy density in terms of argon gas pressure, solenoid voltage, anode voltage, cathode voltage and irradiation distance is obtained as follows:

$$En = (0.9157ca^2 + 2.0188ca)\frac{id \cdot e^{ar^2 - 14.5689ar}}{id^2 + 34.8661id}(1 + 0.02477\ln\frac{an}{2})[1 + (\frac{so - 0.5}{1.5})^{0.35886}] \qquad (2)$$

Equation (2) indicates that the energy density of HCPEB increases with the increase of cathode voltage, but it decreases with the increase of argon gas pressure in the vacuum. The fitted relationship of the energy density to the independent variable at a fixed value of the other five independent variables is shown in Fig. 9. Figure 9 indicates that the voltage of solenoid coil and anode have less effects on the energy density than other three parameters. The cathode voltage and argon gas pressure are two important factors that determine the final energy density of the electron beams. The anode voltage has smallest effect on the energy density. All these are in good agreement with experimental results.
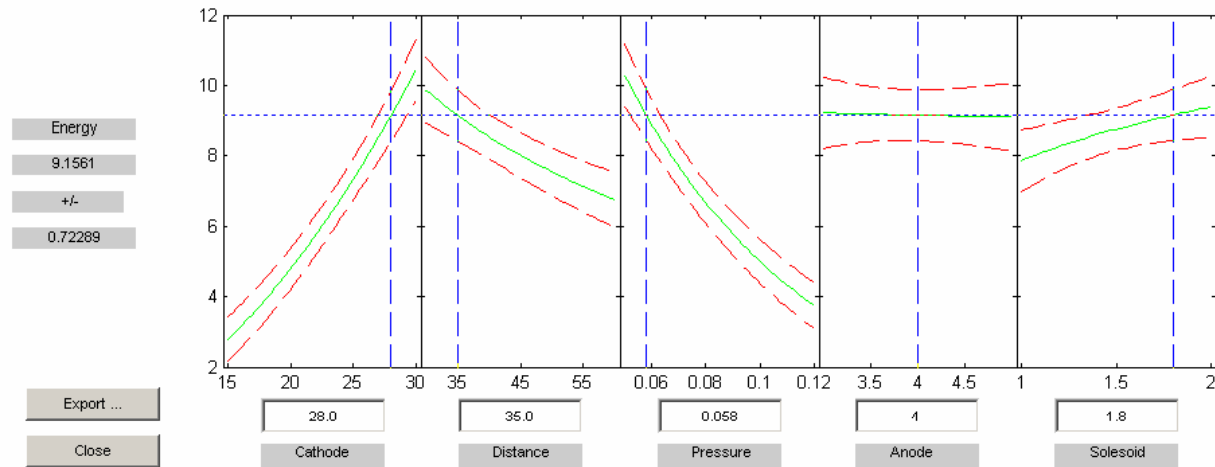

Fig. 9 Fitted relationship of the energy density to the independent variable at fixed values of the other four independent variables

Further experiments have been carried out to verify the fitted model. The histogram of the difference between the experimental energy densities and the calculated ones is shown in Fig. 10.

16

It appears that the difference distributed normally. In order to check the distribution of the difference between the experimental values and calculated ones, a normal distribution plot is used, as shown in Fig. 11. Within the range of probabilities between 0.03 and 0.80, the plot is linear, which indicates that the difference between the experimental energy densities and the calculated ones almost has a normal distribution. This difference may come from the normal distributed error in the measuring process. Therefore, this fitted model has a good accuracy.
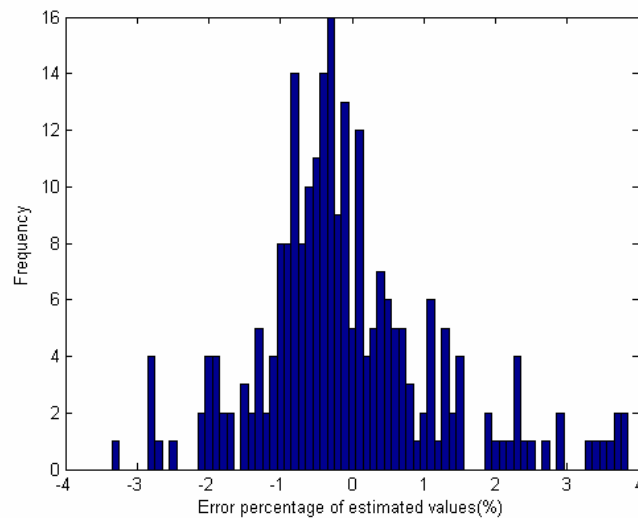

Fig. 10 Histogram of the difference between experimental and estimated values of energy densities

5. Conclusions

The HCPEB irradiation will be a new potential method for machining hard steels and alloys. But there is only limited knowledge regarding its properties. In this paper, the formation process and energy density of HCPEB are studied. Based on the images captured during the plasma formation process with high-speed CCD cameras, the plasma is first generated near the anode wall, then distributes uniformly inside the plasma generation chamber. Experiments also indicate that larger argon gas pressure results in the non-uniformly plasma, and a median value of solenoid voltage is helpful to generate a uniform HCPEB with certain energy density. In

17

addition, a calorimeter is used to measure the energy density, and a mathematical model is fitted

with nonlinear regression to describe the relationship between five dominant beam conditions

with the energy density of HCPEB. By comparing the estimated values with the experimental

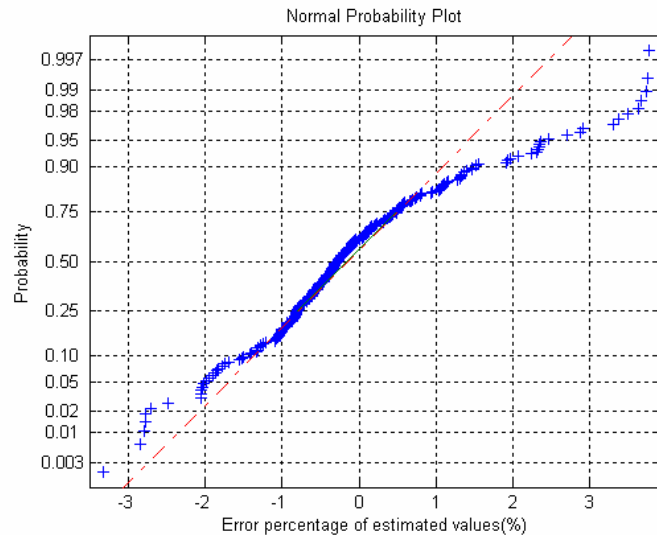results, it is found that this fitted model has a good accuracy.

Fig. 11 A normal probability plot of the difference between experimental and estimated values

of energy densities

References:

[1] Proskurovsky DI, Rotshtein VP, Ozur GE (1997) Surf Coat Tech 96:117

[2] Ivanov Yu, Matz W, Rotshtein V, Günzel R, Sevchenko N (2002) Surf Coat Tech 150:188

[3] Yu Z, Wang ZG, Yamazaki K, Sano S (2006) J Mater Process Tech 180:246

[4] Bretagne J, Delouya G, Godart J, Puech V (1981) J Phys D: Appl Phys, 14:1225

[5] Sigeneger F, Winkler R (2005) Plasma Chemistry and Plasma Processing, 25:147

[6] Konstantinov VO, Khmel SY (2007) J Appl Mech Technical Phys, 48:1

[7] Ozur GE, Proskurovsky DI, Rotshtein VP, Markov AB (2003) Laser & Particle Beams,

21/2:157.

[8] Proskurovsky DI, Rotshtein VP, Ozur GE, Markov AB, Nazarov DS et al. (1998), J. Vac. Sci. Technol. A, 16/4:2480

[9] Myers RH, Montgomery DC (1995) Response surface methodology: process and product optimization using designed experiments, Wiley, New York, p 279-350

[10] Baguer N, Bogaerts A, Gijbels R (2003) J Appl Phys, 94:2212

[11] Motulsky HJ, Christopoulos A (2004) Fitting models to biological data using linear and nonlinear regression: A practical guide to curve fitting, Oxford University Press, UK, p 13-57

[12] SAS Institute (1985) SAS user's guide: statistics, Cary, N.C., USA, p 3-13